Electronic Supplementary Material (ESI) for Materials Horizons.

Tough sheets of nanowires produced floating in the gas phase

- Supporting information -

Richard S. Schäufele,[†,‡] Miguel Vázquez-Pufleau,[†] and Juan J. Vilatela[*,†]

†*IMDEA Materials, Madrid, 28049, Spain*

‡*Department of Applied Physics, Universidad Autónoma de Madrid, Cantoblanco, 28049, Madrid, Spain*

E-mail: juanjose.vilatela@imdea.org

Comparison of growth rates for SiNWs grown by CVD, including FCCVD

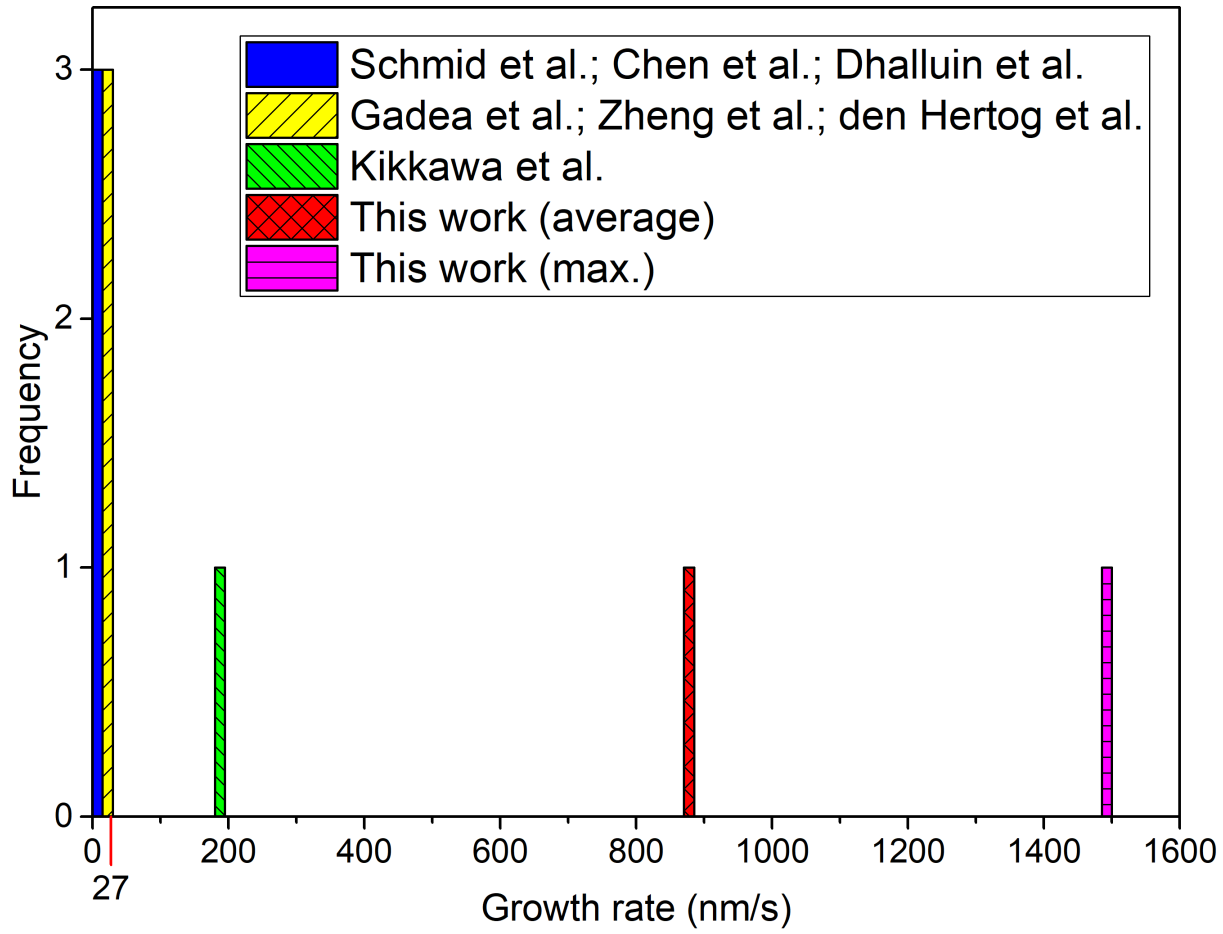

Figure S1: Reported SiNW growth rates for gold-catalysed low pressure CVD (<40mbar)[1–6] and atmospheric pressure CVD[7] using SiH_4 as precursor.

Macroscopic aggregates formed in the gas-phase

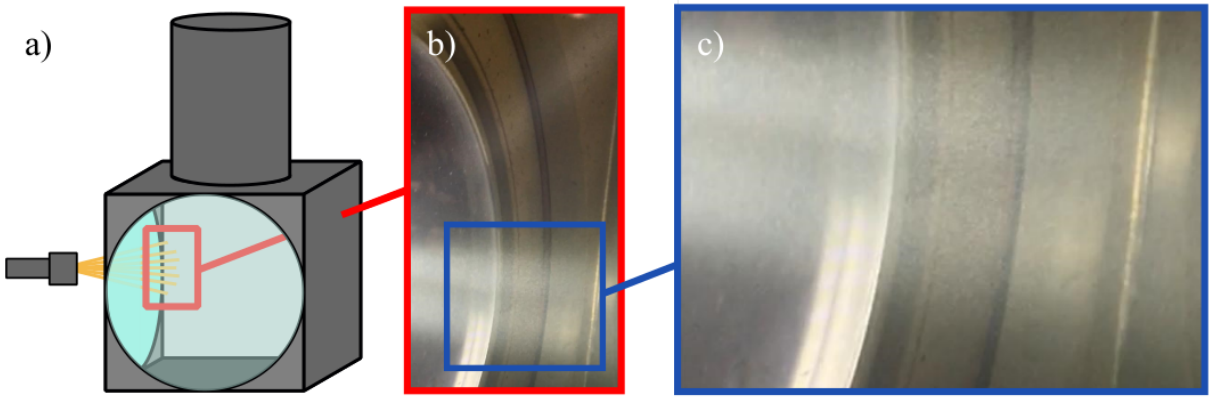

Figure S2: Observation of macroscopic aggregates of SiNWs at the exit of the FCCVD reactor a) Scheme indicating location of samples and where the photograph was taken. b) Photograph showing widespread small macroscopic aggregates floating in the gas phase. c) Higher magnification image of b).

Additional electron micrograph of SiNWs

SiNW diameter distributions were obtained by image analysis of scanning electron micrographs at a magnification of 50k. Figure S3 shows an examples of a typical micrograph used.

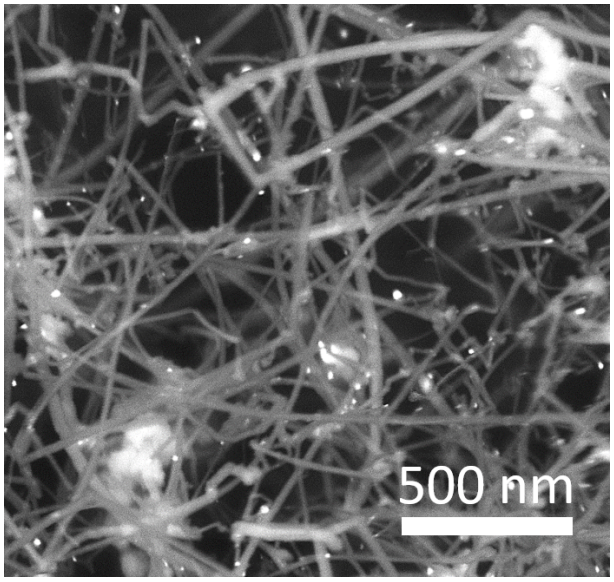

Figure S3: Example of a typical SEM micrograph used for determination of SiNW diameters.

SiNW diameter vs aspect ratio & SiNW diameter vs length

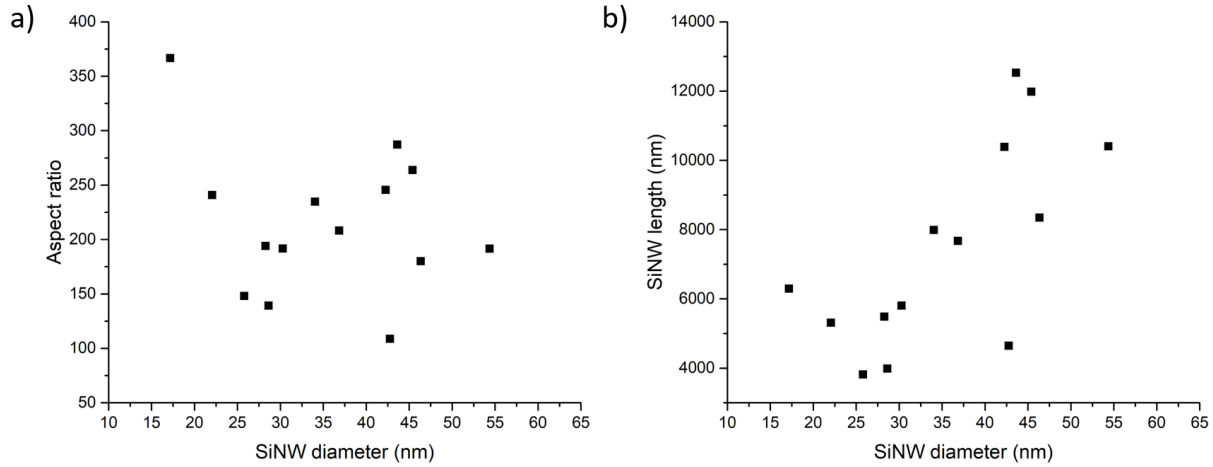

Figure S4: Plots of SiNW diameter versus aspect ratio (a) and length (b), showing that aspect ratio of FCCVD-grown SiNWs is independent of SiNW diameter.

Contact between SiNWs

Small diameter SiNWs can form contact areas, which are effectively domains over which they can transfer stress in shear. Some examples are shown in the electron micrographs in Figure S5.

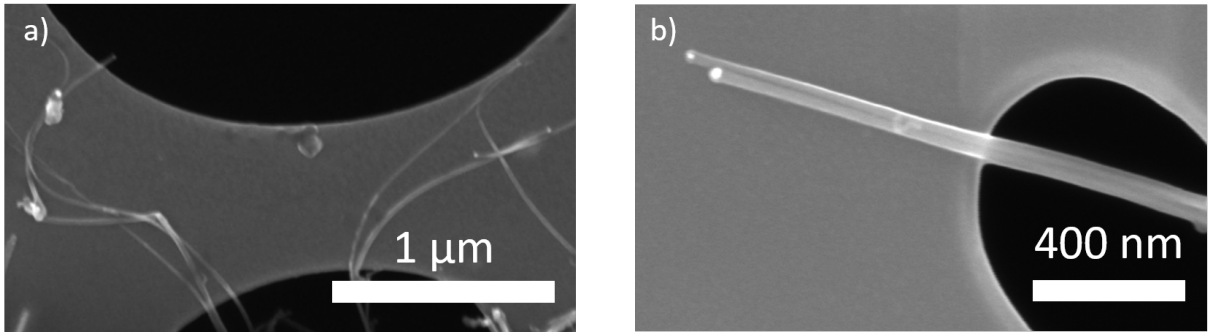

Figure S5: Electron micrographs showing SiNWs forming bundles. The large contact area give rise to high tensile fracture energy in the macroscopic SiNW sheet.

Tensile tests and mechanical data

Table S1: Comparison of tensile properties of 1D nanomaterial ensembles and other porous materials

Composition	Relative density ρ/ρ_{theory}	Density (g/cm^3)	Fracture energy (J/g)	Strength (MPa/SG)	Fracture strain (%)	Reference
SiNW sheet	0.061	0.128	0.18 ± 0.1	12.1 ±3	2.75 ± 0.7	(this work)
CNT-buckypaper	0.28	0.53	0.27	11.9	0.7	[8]
CNT-fibre	0.5	0.5	13	1444	4	[9]
BNNT-buckypaper	0.2	0.4	0.56	7	8	[10]
NF of PAN, SiO_2	0.005	0.008	0.02	0.5	7	[11]
NF of SiO_2	0.002	0.005	0.01	0.8	3.5	[12]
SiO_2 aerogel	0.028	0.075	0.001	0.13	≈ 2	[13]

As an example of bulk Si we consider a Si wafer. Tensile strain-to-break (0.06%) and tensile fracture energy ($0.03X10^6$J/m^3) are calculated from experimental values of tensile strength (102 MPa)[14] and assuming linear elastic behaviour with the modulus of crystalline Si (165.6 GPa).[15] Specific tensile fracture energy comes out as $0.014J/g$. Mechanical data for Si-based electrodes is obtained from reference.[16] For CNT-free electrodes: strength = $0.25MPa$, strain-to-break = 0.35% and tensile fracture energy = $2.5x10^3$J/m^3 ($0.003J/g$). Composite electrodes with 7.5 wt.% carbon nanotubes showing near theoretical capacity have strength = $4.5MPa$, strain-to-break = 5% and tensile fracture energy = $0.15x10^6$J/m^3 ($0.21J/g$).

Comparison of methods for synthesis of 1D inorganic nanostructures

For BNNT, we take an average length of $0.2\mu m$ and average diameter of $6.5nm$,[17] continuous throughput of $20mg/h$ estimated from TEM observations[18] and particle concentration calculated from flow rates for sample N in reference.[17] For CNT fibres, data are from in-house samples produced using IMDEA's FCCVD system under synthesis conditions reported previously.[19] For CNT thin films, data are from reference.[20]

References

(1) Zheng, G.; Lu, W.; Jin, S.; Lieber, C. M. Synthesis and fabrication of high-performance n-type silicon nanowire transistors. *Advanced Materials* **2004**, *16*, 1890–1893.

(2) Gadea, G.; Morata, A.; Santos, J.; Dávila, D.; Calaza, C.; Salleras, M.; Fonseca, L.; Tarancón, A. Towards a full integration of vertically aligned silicon nanowires in MEMS using silane as a precursor. *Nanotechnology* **2015**, *26*, 195302.

(3) Schmid, H.; Björk, M.; Knoch, J.; Riel, H.; Riess, W.; Rice, P.; Topuria, T. Patterned epitaxial vapor-liquid-solid growth of silicon nanowires on Si (111) using silane. *Journal of Applied Physics* **2008**, *103*, 024304.

(4) den Hertog, M. I.; Rouviere, J.-L.; Dhalluin, F.; Desré, P. J.; Gentile, P.; Ferret, P.; Oehler, F.; Baron, T. Control of gold surface diffusion on Si nanowires. *Nano letters* **2008**, *8*, 1544–1550.

(5) Chen, W.; Lardé, R.; Cadel, E.; Xu, T.; Grandidier, B.; Nys, J.; Stiévenard, D.; Pareige, P. Study of the effect of gas pressure and catalyst droplets number density on silicon nanowires growth, tapering, and gold coverage. *Journal of Applied Physics* **2010**, *107*, 084902.

(6) Dhalluin, F.; Baron, T.; Ferret, P.; Salem, B.; Gentile, P.; Harmand, J.-C. Silicon nanowires: Diameter dependence of growth rate and delay in growth. *Applied Physics Letters* **2010**, *96*, 133109.

(7) Kikkawa, J.; Ohno, Y.; Takeda, S. Growth rate of silicon nanowires. *Applied Physics Letters* **2005**, *86*, 123109.

(8) Coleman, J. N.; Blau, W. J.; Dalton, A. B.; Muñoz, E.; Collins, S.; Kim, B. G.; Razal, J.; Selvidge, M.; Vieiro, G.; Baughman, R. H. Improving the mechanical properties of

single-walled carbon nanotube sheets by intercalation of polymeric adhesives. *Applied Physics Letters* **2003**, *82*, 1682–1684.

(9) Koziol, K.; Vilatela, J. J.; Moisala, A.; Motta, M.; Cunniff, P.; Sennett, M.; Windle, A. High-Performance Carbon Nanotube Fiber. *Science* **2007**, *318*, 1892–1895.

(10) Nautiyal, P.; Zhang, C.; Loganathan, A.; Boesl, B.; Agarwal, A. High-Temperature Mechanics of Boron Nitride Nanotube "Buckypaper" for Engineering Advanced Structural Materials. *ACS Applied Nano Materials* **2019**, *2*, 4402–4416.

(11) Si, Y.; Yu, J.; Tang, X.; Ge, J.; Ding, B. Ultralight nanofibre-assembled cellular aerogels with superelasticity and multifunctionality. *Nature Communications* **2014**, *5*.

(12) Si, Y.; Wang, X.; Dou, L.; Yu, J.; Ding, B. Ultralight and fire-resistant ceramic nanofibrous aerogels with temperature-invariant superelasticity. *Science Advances* **2018**, *4*.

(13) Wong, J. C.; Kaymak, H.; Brunner, S.; Koebel, M. M. Mechanical properties of monolithic silica aerogels made from polyethoxydisiloxanes. *Microporous and Mesoporous Materials* **2014**, *183*, 23 – 29.

(14) K. Wasmer, J. M. C. B. M. V. d. M. P. N., A. Bidiville Effect of strength test methods on silicon wafer strengthmeasurements. *Proc. 22nd Eur. Photovolt. Solar Energy Conf., Milan, Italy* **2007**, 1135–1140.

(15) Hopcroft, M. A.; Nix, W. D.; Kenny, T. W. What is the Young's Modulus of Silicon? *Journal of Microelectromechanical Systems* **2010**, *19*, 229–238.

(16) Park, S.-H.; King, P.; Tian, R.; Boland, C.; Coelho, J.; Zhang, C.; McBean, P.; McEvoy, N.; Kremer, M.; Daly, D.; Coleman, J.; Nicolosi, V. High areal capacity battery electrodes enabled by segregated nanotube networks. *Nature Energy* **2019**, *4*, 560–567.

(17) Chatterjee, S.; Kim, M. J.; Zakharov, D. N.; Kim, S. M.; Stach, E. A.; Maruyama, B.; Sneddon, L. G. Syntheses of Boron Nitride Nanotubes from Borazine and Decaborane

Molecular Precursors by Catalytic Chemical Vapor Deposition with a Floating Nickel Catalyst. *Chemistry of Materials* **2012**, *24*, 2872–2879.

(18) Kim, M. J.; Chatterjee, S.; Kim, S. M.; Stach, E. A.; Bradley, M. G.; Pender, M. J.; Sneddon, L. G.; Maruyama, B. Double-Walled Boron Nitride Nanotubes Grown by Floating Catalyst Chemical Vapor Deposition. *Nano Letters* **2008**, *8*, 3298–3302.

(19) Reguero, V.; Alemán, B.; Mas, B.; Vilatela, J. J. Controlling Carbon Nanotube Type in Macroscopic Fibers Synthesized by the Direct Spinning Process. *Chemistry of Materials* **2014**, *26*, 3550–3557.

(20) Mustonen, K. On the limit of single-walled carbon nanotube random network conductivity. Ph.D. thesis, Department of Applied Physics, Aalto University School of Science, 2015.